Theoret. Chim. Acta (Berl.) 66, 261-276 (1984)

THEORETICA CHIMICA ACTA

An LCAO description of the dynamical symmetry in the hydrogen molecular ion

Jens Peder Dahl and Xuejun Feng*

Department of Chemical Physics, Technical University of Denmark, DTH 301, DK-2800 Lyngby, Denmark

The electronic states of one-electron diatomic molecules possess two types of symmetry, geometrical and dynamical. The latter is in general ignored when the LCAO description is adapted. We demonstrate how it can be included, and how its inclusion modifies the ordinary description in regions where states of the same geometrical symmetry cross.

Key words: Hydrogen molecular ion—dynamical symmetry—energy level crossing—molecular orbitals

1. Introduction

The problem of a single electron in the electrostatic field of two fixed nuclei is defined by the Hamiltonian

$$H = -\frac{\hbar^2}{2m}\nabla^2 - \frac{k_a}{r_a} - \frac{k_b}{r_b} \tag{1}$$

where k_a and k_b are the strengths of the two point charges, m is the mass of the electron, and $\hbar$ is Planck's constant divided by 2π. r_a and r_b are the distances from the electron to the two nuclei, whose positions we denote by A and B, respectively. The situation is depicted in Fig. 1 which also defines three appropriate coordinate systems with parallel axes.

The geometrical symmetry of the two-center problem, namely, the rotational invariance about the internuclear axis, involves that the angular momentum λ

* *Permanent address:* Department of Chemistry, Anhui Normal University. Wuhu, Anhui, China

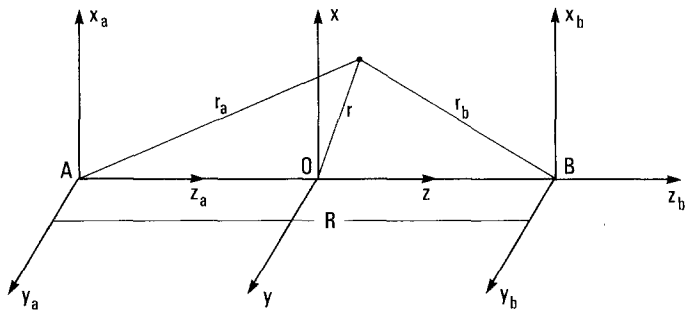

Fig. 1. Coordinate system for diatomic molecules

about that axis is a constant of the motion, i.e. λ commutes with the Hamiltonian (1). Referring to Fig. 1 we have that

$$\lambda = l_{az} = l_{bz} = l_z \tag{2}$$

with l_a, l_b, and l denoting the angular momentum of the electron about the centres A, B, and 0, respectively.

But in addition to the geometrical symmetry represented by λ, the two-centre problem defined by Eq. (1) also possesses dynamical symmetry. The corresponding constant of the motion may be written in any of the three equivalent forms

$$N = \begin{cases} l_a^2 - mR\left(M_{az} + \dfrac{k_b z_b}{r_b}\right) & \text{(3a)} \\ l_b^2 + mR\left(M_{bz} + \dfrac{k_a z_a}{r_a}\right) & \text{(3b)} \\ l^2 - \dfrac{R^2}{4}(p_x^2 + p_y^2) + mR\left(\dfrac{k_a z_a}{r_a} - \dfrac{k_b z_b}{r_b}\right) & \text{(3c)} \end{cases}$$

which refer, respectively, to the coordinate systems centered at A, B, and 0 in Fig. 1. $\boldsymbol{p}$ is the linear momentum of the electron and $\boldsymbol{M}$ denotes the Runge-Lenz vector whose components are constants of the motion in the one-center problem [1, Sect. 30]. Thus

$$\boldsymbol{M}_a = \frac{1}{2m}(\boldsymbol{p}_a \times \boldsymbol{l}_a - \boldsymbol{l}_a \times \boldsymbol{p}_a) - \frac{k_a \boldsymbol{r}_a}{r_a} \tag{4a}$$

$$\boldsymbol{M}_b = \frac{1}{2m}(\boldsymbol{p}_b \times \boldsymbol{l}_b - \boldsymbol{l}_b \times \boldsymbol{p}_b) - \frac{k_b \boldsymbol{r}_b}{r_b}. \tag{4b}$$

The form of N was first discovered and discussed by Erikson and Hill [2]. Their treatment was elaborated by Coulson and Joseph [3] who also extended the definition of N to a space of arbitrary dimension. Both pairs of authors pointed out that the presence of N is tied to the fact that the two-center problem defined by (1) is separable in prolate spheroidal coordinates with A and B as foci.

Subsequently Helfrich [4] constructed constants of the motion for all problems with cylinder symmetry which separate in spheroidal coordinates. Thus, the solutions of the Schrödinger equation

$$H\psi = E\psi \tag{5}$$

may be written in the form

$$\psi_{n_\mu n_\nu m}(\mu, \nu, \phi) = CU(\mu)V(\nu)\exp(im\phi), \qquad m = 0, \pm 1, \pm 2, \ldots \tag{6}$$

where

$$\mu = \frac{r_a + r_b}{R}, \qquad \nu = \frac{r_a - r_b}{R} \tag{7}$$

and ϕ is the angle about the internuclear axis, while C is a normalization constant. The quantum numbers n_μ and n_ν give the number of nodes in $U(\mu)$ and $V(\nu)$, respectively.

Thanks to the separability, the Schrödinger equation (5) can be solved exactly for all values of the internuclear distance R, from the united-atom limit ($R = 0$) to the limit of separated atoms ($R \sim \infty$). The resulting wavefunctions are prototypes of molecular orbitals (MOs) for diatomic molecules and have been much discussed, especially for the homonuclear case. Much attention has also been paid to the so-called correlation diagram, which for a particular choice of nuclear charges shows the variation of the molecular orbital energies as functions of R, between the limits $R = 0$, and $R \sim \infty$. A correlation diagram for the six lowest σ-states of the hydrogen molecular ion H_2^+ is shown in Fig. 2.

The number of paper discussing the solutions (6) is quite large. For references we refer to the comprehensive treatments in Refs. [5–9]. Approximate solutions are reviewed in Refs. [7], [10], and [11].

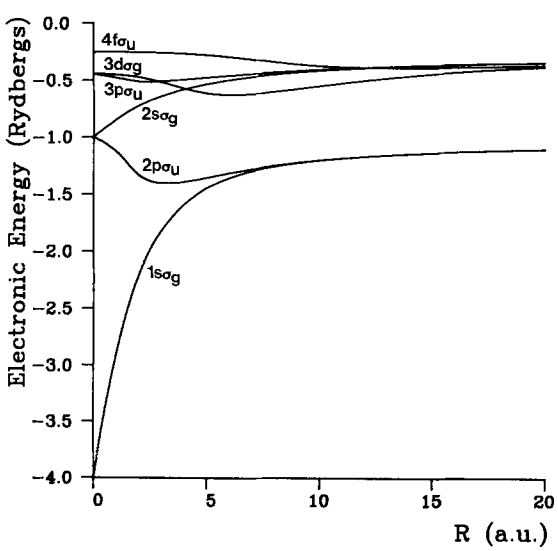

Fig. 2. Some electronic energy levels of H_2^+ as functions of internuclear distance (calculated by Power's one-electron diatomic molecule program [12])

Since the operators defined by (1), (2), and (3) form a commuting set, the exact wavefunctions (6) must be common eigenfunctions of all three operators. Hence, we have, in addition to Eq. (5), that

$$\lambda\psi_{n_\mu n_\nu m} = m\hbar\psi_{n_\mu n_\nu m} \tag{8}$$

and

$$N\psi_{n_\mu n_\nu m} = -A'\psi_{n_\mu n_\nu m}. \tag{9}$$

The eigenvalue $-A'$ is, in atomic units, essentially the μ, ν separation constant obtained by separating Eq. (5) according to the product form (6). Thus, A' is tabulated in, say Refs. [6] and [8], for each of the lower states of H_2^+, as a function of R.

Molecular orbitals for molecules with more than one electron are most often represented as linear combinations of atomic orbitals (LCAOs). Hence, there has also been much interest in LCAO MO approximations to the functions (6), in particular for the low-lying states of H_2^+, [7], [10], [11]. In setting up such approximations one usually assures that Eq. (8) is exactly fulfilled, whereas Eq. (5) is replaced by the variational equation

$$\delta < \psi | H | \psi > = 0. \tag{10}$$

No attempt has been made, however, to include the operator N, and hence Eq. (9), in this type of description.

It is the purpose of the present paper to remedy this situation. We have considered the 8 lowest-lying electronic states of H_2^+ in a fairly simple LCAO MO description and compared calculated values of A' with the exact ones. Special emphasis has been paid to the crossing of energy levels for states with the same m-value. The results of our investigation are presented in the following sections.

2. Characterization of states and basis sets

The H_2^+ electronic states that we have analyzed are those that dissociate to atomic states with the principal quantum number equal to 1 or 2. The general characteristics of these states are listed in Table 1. The central column gives the quantum numbers of the states according to Eq. (6) and the neighbouring columns the quantum numbers in the united-atom and separated-atoms limits. In the united-atom limit the spheroidal coordinates become spherical polar coordinates about 0 (Fig. 1), and in the separated-atoms limit they become parabolic coordinates about A and B. The precise definition of n_1, n_2 and m is then that they are the parabolic quantum numbers at A, in the notation used by Schiff [1, Sect. 16]. The principal quantum number at A (and B) has the value $n_1 + n_2 + |m| + 1$. The connexion between the quantum numbers in these three middle columns is obtained by requiring that the number of nodes be independent of R, as discussed in great detail by Morse and Stueckelberg [13]. See also [9].

The state designation given in the first column of Table 1 is the one usually used for H_2^+ (Fig. 2). It refers, of course, to the quantum numbers in column 4, and to the fact that the electronic states of a homonuclear diatomic molecule are

Table 1. Values of the energy (in Rydbergs), $-A'$ (in a.u.), and the various quantum numbers in the united-atom and the separated-atoms limits

United Atom				Molecule		Separated Atoms		
Designation	$-E$	$-A'$	$nl\|m\|$	$n_\lambda n_\mu\|m\|$	$n_1 n_2\|m\|$	$-A'$	$-E$	Designation
$1s\sigma_g$	4	0	100	000	000	R	1	$\sigma_g 1s$
$2s\sigma_g$	1	0	200	100	100	$R/2$	$\frac{1}{4}$	$\sigma_g 2di^{out}$
$3d\sigma_g$	$\frac{4}{9}$	6	320	020	010	$3R/2$	$\frac{1}{4}$	$\sigma_g 2di^{in}$
$2p\sigma_u$	1	2	210	010	000	R	1	$\sigma_u 1s$
$3p\sigma_u$	$\frac{4}{9}$	2	310	100	100	$R/2$	$\frac{1}{4}$	$\sigma_u 2di^{out}$
$4f\sigma_u$	$\frac{1}{4}$	12	430	030	010	$3R/2$	$\frac{1}{4}$	$\sigma_u 2di^{in}$
$2p\pi_u$	1	2	211	001	001	R	$\frac{1}{4}$	$\pi_u 2p$
$3d\pi_g$	$\frac{4}{9}$	6	321	011	001	R	$\frac{1}{4}$	$\pi_g 2p$

either even or odd (geometrical symmetry). The designation given in the last column is derived from the quantum numbers in column 6 in a self explanatory way. As in Ref. [11], $2di^{in}$ is a digonal hybrid at A with its vertex pointing toward B, $2di^{out}$ is a similar hybrid with its vertex pointing away from B.

The energies in columns 2 and 8 are directly derived from the Balmer formula. The unit of energy is the Rydberg unit, since this is the unit used in the extensive tables of Refs. [6] and [8].

The LCAO MO description of the states of Table 1 is in our work based on the following set of hydrogen-like atomic orbitals on centres A and B,

$$\begin{cases} (1s) = \pi^{-1/2}(2\zeta)^{3/2} \exp(-2\zeta r) \\ (2s) = \pi^{-1/2}\zeta^{3/2}(1-\zeta r) \exp(-\zeta r) \\ (2p_0) = \pi^{-1/2}\zeta^{5/2} r \exp(-\zeta r) \cos\theta \\ (2p_{\pm_1}) = (2\pi)^{-1/2}\zeta^{5/2} r \exp(-\zeta r) \sin\theta \exp(\pm i\phi) \end{cases} \tag{11}$$

where (r, θ, ϕ) are spherical polar coordinates about A and B. The orbital exponent ζ is a variational parameter depending on R and the state considered. With this basis set we can represent the separated-atoms limit correctly for all the states studied here, whereas only the $1s\sigma_g$, $2s\sigma_g$, $2p\sigma_u$, and $2p\pi_u$ states can be correctly represented in the united-atom limit. The basis set is, however, sufficiently flexible for our purpose which is to illustrate how the dynamical symmetry is incorporated in the LCAO MO description.

We shall now consider this description in detail and, for simplicity, we consider the two π states of Table 1 first.

3. The $2p\pi_u$ and $3d\pi_g$ states

With the basis (11), the LCAO MOs of these states are completely determined by the geometrical symmetry, apart from the value of ζ. They are

$$\psi = [2(1 \pm S)]^{-1/2}\{(2p\pi)_a \pm (2p\pi)_b\} \tag{12}$$

where the upper sign refers to the $2p\pi_u$ state, the lower sign to the $3d\pi_g$ state. $(2p\pi)$ is either $2p_1$ on A and B, or $2p_{-1}$ on A and B, and S is the overlap integral,

$$S = \langle (2p_1)_a | (2p_1)_b \rangle. \tag{13}$$

The electronic energies of the states are

$$E = \langle \psi | H | \psi \rangle. \tag{14}$$

Inspired by Slater's discussion of the $1s\sigma_g$ state [7] we write

$$E = \zeta^2 F_1(w) + \zeta F_2(w). \tag{15}$$

with $w = \zeta R$. Further, we measure lengths in atomic units and energies in Rydberg units, and find by standard methods [14]

$$S = e^{-w}(1 + w + \tfrac{2}{5}w^2 + \tfrac{1}{15}w^3) \tag{16}$$

$$F_1 = (1 \pm S)^{-1}\{1 \pm e^{-w}(1 + w + \tfrac{4}{15}w^2 - \tfrac{1}{15}w^3)\} \tag{17}$$

$$F_2 = -(1 \pm S)^{-1}\left\{1 + \frac{2}{w} - \frac{3}{w^3} + e^{-2w}\left(1 + \frac{4}{w} + \frac{6}{w^2} + \frac{3}{w^3}\right) \pm 2e^{-w}(1 + w + \tfrac{1}{3}w^2)\right\}. \tag{18}$$

Again, the upper sign refers to the $2p\pi_u$ state and the lower sign to the $3d\pi_g$ state.

Minimization of the expression (15) with respect to ζ at fixed internuclear distance gives

$$\zeta = -\frac{F_2 + w dF_2/dw}{2F_1 + w dF_1/dw}. \tag{19}$$

By solving this equation with R as a parameter we obtain the MOs (12) and energies (14) as functions of R. The results are shown in Tables A.6 and A.7 for some selected values of R, together with the exact energies, E(exact).

Also shown in Tables A.6 and A.7 is $-A'$ (exact), as obtained from the separation constant in spheroidal coordinates. It is the exact eigenvalue of Eq. (9) and represents the dynamical symmetry of the problem. In the LCAO MO method we approximate it with the expectation value of N,

$$-A' = \langle \psi | N | \psi \rangle. \tag{20}$$

The closer agreement there is between the values of $-A'$ and $-A'$ (exact), the better does the approximate wavefunction reflect the dynamical symmetry.

The $-A'$ values calculated from Eq. (20) are also given in Tables A.6 and A.7, and we see that the simple wavefunctions (12) in fact give a fairly good representation of the dynamical symmetry for all values of R, for both π states. As pointed out in the previous section we cannot obtain a correct wavefunction for the $3d\pi_g$ state as R tends to zero, and this is reflected in the calculated E values. However, the minus combination in (12) does become a d function at $R = 0$, and hence it gives the correct limiting value for the eigenvalue of N.

The favorable agreement between the values of $-A'$ and $-A'$ (exact) for the $2p\pi_u$ and $3d\pi_g$ states shows, that it is meaningful to talk about dynamical symmetry also for approximate wavefunctions. The dynamical symmetry itself becomes in this way less esoteric, and the meaning of the separation constant in spheroidal coordinates becomes more transparent.

The actual evaluation of integrals containing the operator N, like the integral in Eq. (20), will be discussed in the Appendix.

4. The σ_g and σ_u states

The basis (11) allows us to construct three σ_g states and three σ_u states. They have the general form

$$\psi = \{c_1(1s)_a + c_2(2s)_a + c_3(2p_0)_a\} \pm \{c_1(1s)_b + c_2(2s)_b - c_3(2p_o)_b\} \tag{21}$$

where the upper sign refers to the σ_g states and the lower sign to the σ_u states.

Applying the variational equation (10) for each value of R leads to the energy ordered states $1\sigma_g$, $2\sigma_g$, $3\sigma_g$ and $1\sigma_u$, $2\sigma_u$, $3\sigma_u$. Each of these states is characterized by an orbital exponent $\zeta(R)$ and a set of coefficients $c_i(R)$. To determine them we have solved the secular equation

$$\boldsymbol{Hc} = \boldsymbol{ScE} \tag{22}$$

as a function of ζ for each R value, and then assigned ζ values to states such that the energy of each state becomes as low as possible. (In Eq. (22) $\boldsymbol{H}$ is the matrix of the Hamiltonian, $\boldsymbol{S}$ the overlap matrix, $\boldsymbol{E}$ the matrix of eigenvalues and $\boldsymbol{c}$ the matrix of eigenvectors.)

Having determined the LCAO MOs in this way we have next used Eq. (20) for each state to obtain the expectation values of N as functions of R.

The results of these calculations are presented and evaluated in Tables A.1–A.5 and in Figs. 3 and 4.

Thus, Table A.1 compares the $1\sigma_g$ results with the exact $1s\sigma_g$ results. It shows that the LCAO MO gives a very good description of the ground state, both for the energy and the dynamical symmetry. Similarly, Table A.4 shows that the $1\sigma_u$ function gives a very good picture of the $2p\sigma_u$ state.

The $2\sigma_g$ and $3\sigma_g$ results are less satisfactory in so far as they fail to give a correct representation of the crossing between the $2s\sigma_g$ and the $3d\sigma_g$ energy levels at $R = 4.05$ a.u.

In fact, the LCAO calculations predict an avoided crossing, as shown in Fig. 3. Furthermore the $2\sigma_g$ and $3\sigma_g$ expectation values of N, plotted as functions of R, change rapidly and actually cross in the region where the avoided crossing of the energy levels occurs. This is shown in Fig. 4.

Away from the crossing region the LCAO description gives a qualitatively correct representation of the $2s\sigma_g$ and $3d\sigma_g$ states, except for the $3d\sigma_g$ state at small R,

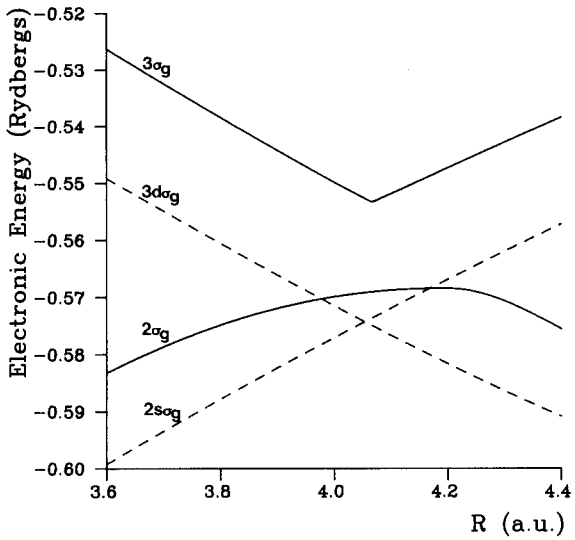

Fig. 3. Energy curves of the $2s\sigma_g$ and the $3d\sigma_g$ states in the crossing region. Solid curves, LCAO MO calculations. Dashed curves, exact calculations

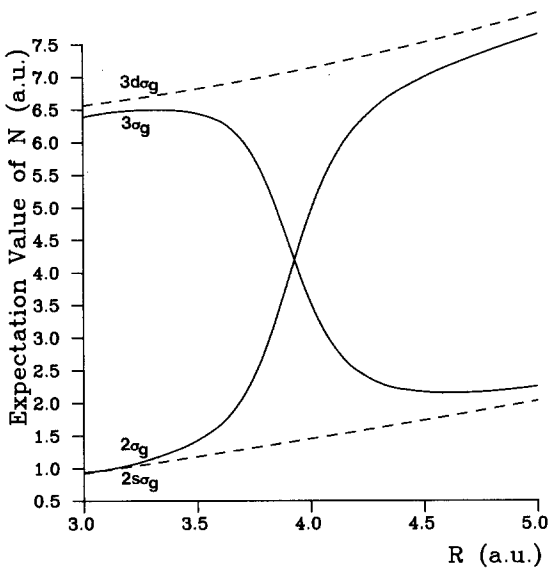

Fig. 4. Values of $-A'$ for the $2s\sigma_g$ and the $3d\sigma_g$ states in the energy crossing region. Solid curves, LCAO MO calculations. Dashed curves, exact values

where A' approaches the wrong limiting value. This is shown in Tables A.2 and A.3.

The unsatisfactory LCAO behavior of A' for the $3d\sigma_g$ state at small R values could easily be removed by adding a $3d$ function to the basis set (11). The

situation at the crossing point is much more difficult to restore. We shall discuss it further in the next section.

Table A.5 analyses the LCAO description of the $3p\sigma_u$ state. Satisfactory results are obtained both for E and A' except in the region where the $3p\sigma_u$ and $4f\sigma_u$ energy levels cross (See Fig. 2). The situation about this crossing point is similar to the situation described above, and hence we shall not discuss it further.

The $4f\sigma_u$ state can not be adequately represented with the basis set (11) because of two level crossings. Besides crossing the $3p\sigma_u$ level at large R, the $4f\sigma_u$ level crosses the $4p\sigma_u$ level at small R. For this reason no table is presented for the $4f\sigma_u$ state.

5. The $2s\sigma_g$, $3d\sigma_g$ energy level crossing

The behavior of the exact and the approximate energy curves in the crossing region (Fig. 3) is easily understood in the light of the noncrossing rule for diatomic molecules [15], according to which energy levels of the same symmetry will not cross when the internuclear separation is varied.

To apply this rule correctly all symmetries of the problem must be included [3]. The $2s\sigma_g$ and the $3d\sigma_g$ states have the same geometrical symmetry, but they differ with respect to dynamical symmetry, as the A' values in Tables A.2 and A.3 show. Hence, the crossing of the exact energy curves does not contradict the noncrossing rule.

The avoided crossing of the LCAO curves reflects the fact that the small basis set (11) is unable to give an exact representation of the dynamical symmetry in the crossing region. In a terminology due to Hatton [16] we may say, that the basis set symmetry only includes the geometrical symmetry. Accordingly, the $2\sigma_g$ and the $3\sigma_g$ energy curves cannot cross.

The noncrossing rule is intimately tied to the variational Eq. (10), i.e. the Hamiltonian is given a preferred status. It may, however, be argued that the operators H and N should be treated on the same footing, especially in the crossing region. In the LCAO description this is tantamount to saying that the matrices of H and N, as defined by the basis set (11), should play equal roles in the determination of the LCAO MOs.

The LCAO coefficients determined from (10) are eigenvectors of the H matrix. They would also be eigenvectors of the N matrix if the basis set were complete. But since this is not the case the H and the N matrices fail to commute, and hence they cannot be simultaneously diagonalized. In other words, they cannot lead to one common set of LCAO MOs.

Accordingly, it becomes of interst to consider two different LCAO solutions in the crossing region, one obtained by diagonalizing the H matrix, the other obtained by diagonalizing the N matrix. We have determined such solutions by using the basis set (11) defined by the ζ values from the original $3\sigma_g$ calculation. The results are shown in Figs. 5–7.

Thus, Fig. 5 shows the $2\sigma_g$ and $3\sigma_g$ energy levels obtained by diagonalizing the H matrix. The $3\sigma_g$ curve is the same as in Fig. 3, but the $2\sigma_g$ curve lies above that of Fig. 3 since the ζ values are optimized for the $3\sigma_g$ curve, and not for the $2\sigma_g$ curve.

In Fig. 6 we show the energy curves obtained by first diagonalizing the N matrix, and then calculating the expectation value of H from the eigenvectors of N. It

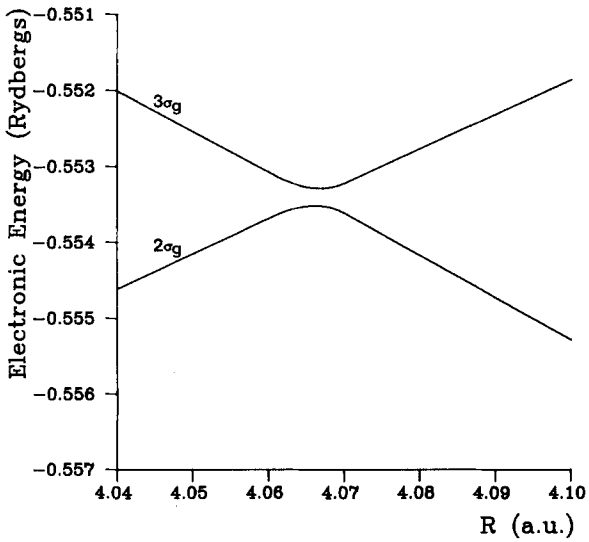

Fig. 5. Energy curves of the $2\sigma_g$ and $3\sigma_g$ states in the crossing region, as obtained by diagonalizing the common H matrix

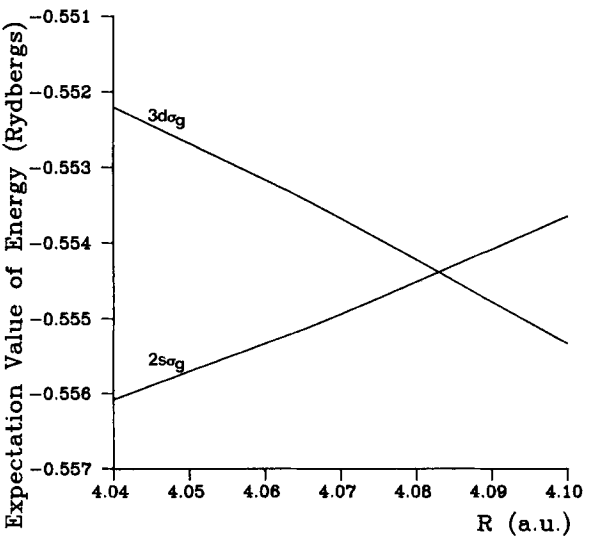

Fig. 6. Energy curves of the $2\sigma_g$ and $3\sigma_g$ states in the crossing region, as obtained by diagonalizing the common N matrix

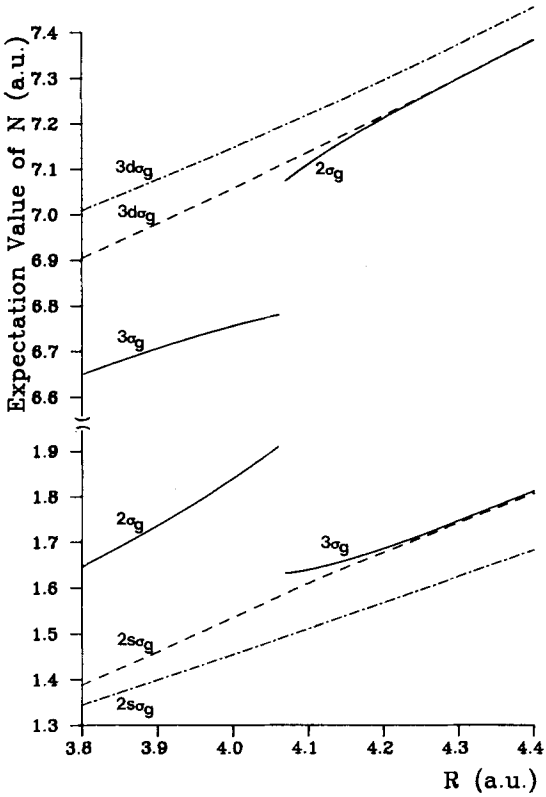

Fig. 7. Values of $-A'$ in the $2s\sigma_g$, $3d\sigma_g$ crossing region. Solid curves from the diagonalization of the common H matrix. Dashed curves from the diagonalization of the common N matrix. Dashed and dotted curves, exact values

is seen that these new energy curves cross in much the same way as the exact ones do.

The A' values obtained by diagonalizing the N matrix are shown in Fig. 7 together with the exact values. The two resulting curves are seen to be almost identical. Also shown in Fig. 7 are the expectation values of N obtained by diagonalizing the H matrix. As in Fig. 4 a rapid variation occurs in the crossing region.

Thus it appears that we obtain the best qualitative behavior of the energy levels in the crossing region by diagonalizing the N matrix rather than the H matrix.

A similar result is obtained for the LCAO description of the $3p\sigma_u$ and $4f\sigma_u$ states in the region where the exact curves cross.

6. Conclusion

The electronic wavefunctions of the hydrogen molecular ion are prototypes of molecular orbitals for homonuclear diatomic molecules, and there has accordingly

been much interest in the LCAO MO description of these functions. In fact, most elementary textbooks in quantum chemistry include a discussion of this description. Such discussions tend, however, to ignore the dynamical symmetry of the problem. The inclusion of this symmetry is necessary in order to account for the crossing of energy curves for states of the same geometrical symmetry.

Since this is by now rather well known, we have found it of importance to demonstrate that it is quite straightforward to incorporate the dynamical symmetry in the LCAO description. Accordingly, we have presented a set of tables and a series of figures in which not only the energy but also the dynamical symmetry is analysed, for the lower electronic states of H_2^+, in both the LCAO and the exact description.

The result of our analysis is that even fairly simple LCAO wavefunctions account well for the dynamical symmetry. In order to obtain a qualitatively correct behaviour in the critical crossing regions it is, however, necessary to diagonalize the dynamical symmetry operator rather than the Hamiltonian.

Acknowledgment The authors want to thank Dr. Helge Johansen for valuable discussions.

Appendix 1. The matrix elements of N

For a given LCAO MO, the expectation value of N is a linear combination of matrix elements of the type

$$N_{ij} = \langle \phi_i | N | \phi_j \rangle \tag{A.1}$$

where ϕ_i and ϕ_j are atomic orbitals of the form (11), at either A or B. The evaluation of N_{ij} is facilitated by the fact that these orbitals have been chosen to be hydrogen-like.

Let us assume that ϕ_j is located at B, and that its l quantum number is l_b. We adopt the expression (3b) for N, with $k_a = k_b = 1$ and the electron mass $m = 1$ (atomic units), and get:

$$\begin{aligned} N_{ij} &= \langle \phi_i | l_b^2 + R M_{bz} + R \frac{z_a}{r_a} | \phi_j \rangle \\ &= l_b(l_b+1)\langle \phi_i | \phi_j \rangle + R \langle \phi_i | M_{bz} | \phi_j \rangle + R \langle \phi_i | \frac{z_a}{r_a} | \phi_j \rangle. \end{aligned} \tag{A.2}$$

To evaluate the integral $\langle \Phi_i | M_{bz} | \phi_j \rangle$ we write ϕ_j as a linear combination of hydrogen-like orbitals in parabolic coordinates and take advantage of the fact that these new orbitals are eigenfunctions of $M_b(\zeta)$, where $M_b(\zeta)$ is obtained from Eq. (4b) by replacing $k_b = 1$ with $k_b = \zeta$. We write accordingly

$$\langle \phi_i | M_{bz} | \phi_j \rangle = \langle \phi_i | M_{bz}(\zeta) | \phi_j \rangle + \langle \phi_i \left| \frac{\zeta - 1}{r_b} \right| \phi_j \rangle \tag{A.3}$$

and reduce the first integral on the right hand side to a linear combination of overlap integrals. The remaining integrals in (A.2) and (A.3) are then evaluated by elementary means [14].

If ϕ_j is located on A rather than B we adopt the expression (3a) for N and proceed in a similar fashion as above.

In closing, we note that one-center matrix elements of M between hydrogenic or Slater type orbitals have been discussed elsewhere by Lohr [17].

Appendix 2. The lower states of the H_2^+ ion

Table A.1. The $1s\sigma_g$ state

R[a]	ζ	$-E$[a]	$-E$ (exact)[b]	$-A'$[a]	$-A'$ (exact)[b]
0.2	0.96816	3.856734	3.857241	0.02576	0.025693
0.4	0.91661	3.598297	3.601508	0.09647	0.095731
1.0	0.77445	2.886848	2.903573	0.48288	0.475947
2.0	0.62926	2.182063	2.205268	1.40439	1.393539
3.0	0.55767	1.804247	1.821792	2.46293	2.458030
4.0	0.52326	1.581482	1.592170	3.56829	3.569090
5.0	0.50829	1.443141	1.448841	4.67458	4.677560
6.0	0.50277	1.354478	1.357271	5.75899	5.761839
8.0	0.50050	1.254489	1.255141	7.85476	7.856078
10.0	0.50016	1.200957	1.201157	9.89517	9.895643
12.0	0.50001	1.166917	1.167003	11.91546	11.915635
14.0	0.49996	1.142950	1.142995	13.92820	13.928273
16.0	0.49996	1.125047	1.125073	15.93734	15.937380
18.0	0.49998	1.111139	1.111155	17.94436	17.944381
20.0	0.49999	1.100018	1.100029	19.94995	19.949961

[a] Energies in Rydbergs, R and $-A'$ in atomic units.
[b] Exact values calculated by Power's one-electron diatomic molecule program [14]

Table A.2. The $2s\sigma_g$ state[a]

R	ζ	$-E$	$-E$ (exact)	$-A'$	$-A'$ (exact)
0.2	0.97970	0.981772	0.981910	0.00669	0.006545
0.4	0.94456	0.947305	0.948199	0.02683	0.025264
1.0	0.84473	0.839683	0.845849	0.16626	0.140308
2.0	0.73255	0.707030	0.721730	0.60716	0.473264
3.0	0.67077	0.620054	0.637774	1.26207	0.924837
4.0	0.69936	0.569866	0.577030	3.89452	1.454587
5.0	0.57416	0.513988	0.531012	2.21444	2.034821
6.0	0.55808	0.480957	0.495109	2.85847	2.644476
8.0	0.53721	0.434771	0.443555	4.08445	3.889907
10.0	0.52625	0.404434	0.409421	5.24557	5.106172
12.0	0.51993	0.383062	0.385836	6.35685	6.265908
14.0	0.51582	0.367136	0.368727	7.43487	7.376319
16.0	0.51288	0.354743	0.355709	8.49218	8.453325
18.0	0.51068	0.344780	0.345404	9.53662	9.509613
20.0	0.50898	0.336574	0.336999	10.57273	10.553066

[a] The LCAO MO results above the broken line are from the $2\sigma_g$ calculation, those below the line from the $3\sigma_g$ calculation

Table A.3. The $3d\sigma_g$ state[a]

R	ζ	$-E$	$-E$ (exact)	$-A'$	$-A'$ (exact)
0.2	0.45003	0.426366	0.444671	4.80697	6.002118
0.4	0.44725	0.425320	0.445355	4.84324	6.008486
1.0	0.44074	0.424574	0.450369	5.02494	6.053745
2.0	0.45442	0.442240	0.471555	5.48778	6.226856
3.0	0.50430	0.489265	0.515009	6.11194	6.566134
4.0	0.57405	0.549843	0.571448	6.75547	7.146648
5.0	0.56115	0.595667	0.612026	7.86651	7.991630
6.0	0.57723	0.609625	0.624990	8.99074	9.057206
8.0	0.56527	0.584123	0.597023	11.56529	11.629215
10.0	0.53808	0.535515	0.546235	14.44758	14.530592
12.0	0.51242	0.488526	0.497326	17.49196	17.592475
14.0	0.49335	0.448907	0.455970	20.62669	20.733189
16.0	0.48191	0.417005	0.422505	23.80926	23.906713
18.0	0.47755	0.391935	0.396058	27.00624	27.082437
20.0	0.47847	0.372586	0.375532	30.18838	30.239564

[a] The LCAO MO results above the broken line are from the $3\sigma_g$ calculation, those below the line from the $2\sigma_g$ calculation

Table A.4. The $2p\sigma_u$ state

R	ζ	$-E$	$-E$ (exact)	$-A'$	$-A'$ (exact)
0.2	1.00297	1.005351	1.005355	2.00403	2.004021
0.4	1.01085	1.021500	1.021568	2.01653	2.016334
1.0	0.73090	1.129041	1.129627	2.11550	2.112417
2.0	0.39931	1.333608	1.335069	2.52183	2.521958
3.0	0.46628	1.402610	1.402837	3.19663	3.196382
4.0	0.48789	1.390840	1.391101	4.02668	4.025941
5.0	0.49672	1.354217	1.354583	4.94204	4.941274
6.0	0.50000	1.314249	1.314621	5.90409	5.903660
8.0	0.50109	1.246974	1.247212	7.89059	7.890707
10.0	0.50080	1.199679	1.199802	9.90274	9.902955
12.0	0.50049	1.166718	1.166782	11.91689	11.917051
14.0	0.50028	1.142924	1.142960	13.92844	13.928532
16.0	0.50015	1.125045	1.125067	15.93737	15.937426
18.0	0.50008	1.111140	1.111154	17.94436	17.944389
20.0	0.50004	1.100019	1.100028	19.94994	19.949962

Table A.5. The $3p\sigma_u$ state[a]

R	ζ	$-E$	$-E$ (exact)	$-A'$	$-A'$ (exact)
0.2	0.54311	0.445239	0.446026	2.00178	2.001784
0.4	0.55012	0.450071	0.450738	2.00721	2.007210
1.0	0.58463	0.478090	0.478631	2.04799	2.047765
2.0	0.62077	0.510382	0.510826	2.20394	2.202550
4.0	0.58335	0.488437	0.490219	2.76422	2.758480
6.0	0.55216	0.452635	0.454865	3.54456	3.527399
8.0	0.53845	0.422965	0.424967	4.45949	4.426124
10.0	0.52890	0.399520	0.401172	5.44327	5.400450
11.0	0.52531	0.389739	0.391204	5.95728	5.904292
12.0	0.52102	0.381020	0.382320	6.46794	6.414889
13.0	0.51909	0.373261	0.374383	6.95950	6.929890
14.0	0.51693	0.366304	0.367272	7.47672	7.447540
16.0	0.51350	0.354405	0.355118	8.51150	8.486053
18.0	0.51099	0.344644	0.345167	9.54526	9.524237
20.0	0.50913	0.336520	0.336905	10.57651	10.559464

[a] The LCAO MO results above the broken line are from the $2\sigma_u$ calculation, those below the line from the $3\sigma_u$ calculation

Table A.6. The $2p\pi_u$ state

R	ζ	$-E$	$-E$ (exact)	$-A'$	$-A'$ (exact)
0.2	0.99739	0.997374	0.997377	2.00799	2.007979
0.4	0.99011	0.989892	0.989932	2.03178	2.031671
1.0	0.95006	0.947277	0.948216	2.19270	2.189385
2.0	0.86016	0.851814	0.857544	2.71070	2.682595
3.0	0.77419	0.761525	0.772888	3.44626	3.376713
4.0	0.70439	0.686450	0.701649	4.31536	4.206448
5.0	0.65044	0.625775	0.642770	5.26895	5.131657
6.0	0.60924	0.576723	0.593983	6.27937	6.125876
8.0	0.55420	0.503851	0.519021	8.40809	8.250623
10.0	0.52375	0.453759	0.465433	10.61442	10.47479
12.0	0.50877	0.418428	0.426569	12.86428	12.72649
14.0	0.50286	0.393007	0.398254	15.04143	14.95673
16.0	0.50128	0.374294	0.377505	17.19950	17.14085
18.0	0.50117	0.360102	0.362037	19.31487	19.27649
20.0	0.50131	0.348979	0.350167	21.39811	21.37357

Table A.7. The $3d\pi_g$ state

R	ζ	$-E$	$-E$ (exact)	$-A'$	$-A'$ (exact)
0.2	0.42951	0.428975	0.444557	6.00245	6.002540
0.4	0.43196	0.430032	0.444892	6.00983	6.010168
1.0	0.44503	0.435551	0.447113	6.06218	6.063825
2.0	0.47519	0.447150	0.453399	6.25476	6.258285
3.0	0.50469	0.456265	0.459371	6.58283	6.586452
4.0	0.52682	0.460253	0.461907	7.04045	7.042433
5.0	0.53999	0.459116	0.460228	7.61259	7.611205
6.0	0.54558	0.454063	0.455078	8.28056	8.274369
8.0	0.54314	0.437521	0.438783	9.83327	9.816631
10.0	0.53380	0.418348	0.419834	11.58362	11.56030
12.0	0.52418	0.400048	0.401550	13.45710	13.43219
14.0	0.51642	0.383815	0.385176	15.40645	15.38344
16.0	0.51082	0.369865	0.371010	17.40084	17.38126
18.0	0.50705	0.358034	0.358952	19.41990	19.40401
20.0	0.50463	0.348039	0.348753	21.45063	21.43808

References

1. Schiff, L. I.: Quantum mechanics, Third Edition. New York: McGraw-Hill 1968
2. Erikson, H. A., Hill, E. L.: Phys. Rev. **75**, 29 (1949)
3. Coulson, C. A., Joseph, A.: Int. J. Quantum Chem. **1**, 337 (1967)
4. Helfrich, K.: Theoret. Chim. Acta (Berl.) **24**, 271 (1972)
5 Hartmann, H., Helfrich, K.: Theoret. Chim. Acta (Berl.) **10**, 406 (1968)
6. Bates, D. R., Ledsham, K., Stewart, A. L.: Philos. Trans. Roy. Soc. A **246**, 215 (1953)
7. Slater, J. C.: Quantum theory of molecules and solids, Vol. 1, Electronic structure of molecules, Chap. 1. New York: McGraw-Hill 1963
8. Teller, E., Sahlin, H. L.: The hydrogen molecular ion and the general theory of electron structure, in: Eyring, H., Henderson, D., Jost, W.: Physical chemistry, an advanced treatment, Vol. V. Valency. New York: Academic Press 1970
9. Helfrich, K., Hartmann, H.: Theoret. Chim. Acta (Berl.) **16**, 263 (1970)
10. Hurley, A. C.: Introduction to the electron theory of small molecules, Chap. 3 New York: Academic Press 1976
11. Mulliken, R. S., Ermler, W. C.: Diatomic molecules. Results of *ab initio* calculations, Chap. II. New York: Academic Press 1977
12. Power, J. D.: Philos Trans. Roy. Soc. A **274**, 663 (1973); Program OEDM (QCPE-233), available from Quantum Chemistry Program Exchange, Indiana University, Bloomington, Indiana 47405, U.S.A.
13. Morse, P. M., Stueckelberg, E. C. G.: Phys. Rev. **33**, 932 (1929)
14. Kotani, M., Amemiya, A., Ishiguro, E., Kimura, T.: Tables of molecular integrals. Tokyo: Maruzen 1963
15. Landau, L. D., Lifshitz, E. M.: Quantum mechanics, Non-relativistic theory, §76. New York: Pergamon Press 1958
16. Hatton, G. J.: Phys. Rev. A **14**, 901 (1976)
17. Lohr, L. L.: Int. J. Quantum Chem. **10**, 799 (1976)

Received May 3, 1984